Transformed Eulerian-Mean Theory. Part II: Potential Vorticity Homogenization and the Equilibrium of a Wind- and Buoyancy-Driven Zonal Flow

ALLEN KUO, R. ALAN PLUMB, AND JOHN MARSHALL

Program in Atmospheres, Oceans and Climate, Department of Earth, Atmospheric and Planetary Sciences, Massachusetts Institute of Technology, Cambridge, Massachusetts

(Manuscript received 14 October 2003, in final form 1 July 2004)

ABSTRACT

The equilibrium of a modeled wind- and buoyancy-driven, baroclinically unstable, flow is analyzed using the transformed Eulerian-mean (TEM) approach described in Part I. Within the near-adiabatic interior of the flow, Ertel potential vorticity is homogenized along mean isopycnals—a finding readily explained using TEM theory, given the geometry of the domain. The equilibrium, zonal-mean buoyancy structure at the surface is determined entirely by a balance between imposed surface fluxes and residual mean and eddy buoyancy transport within a "surface diabatic layer." Balance between these same processes and the wind stress determines the stratification, and hence potential vorticity, immediately below this layer. Ertel potential vorticity homogenization below then determines the mean buoyancy structure everywhere. Accordingly, the equilibrium structure of this flow can be described—and quantitatively reproduced—from knowledge of the eddy mixing rates within the surface diabatic zone and the depth of this zone, together with potential vorticity homogenization beneath. These results emphasize the need to include near-surface buoyancy transport, as well as interior PV transport, in eddy parameterization schemes. They also imply that, in more realistic models, the surface buoyancy balances may be impacted by processes in remote locations that allow diapycnal flow.

1. Introduction

In Part I (Plumb and Ferrari 2005) a nongeostrophic transformed Eulerian-mean (TEM) theory was presented for analysis of eddy transport on a zonal-mean flow. Here, we revisit a problem explored by Karsten et al. (2002, hereinafter KJM), considering the modeled equilibrium state of fluid in a cylindrical tank, forced at its top surface by applied stresses and buoyancy fluxes, in order to illustrate and to explore further the implications of that theory. The model set up is briefly described in section 2. The flow becomes baroclinically unstable and eventually equilibrates to produce a stratified mean state, as shown by KJM and in Fig. 1a, described below. This equilibrium state is described in terms of conventional eddy transports in section 3; aside from the buoyancy structure, other features of interest are the homogenization of mean Ertel potential vorticity (PV) along the mean isopycnals, and the eddy fluxes of buoyancy and of PV, both of which are "skew" (directed along the mean contours of buoyancy and PV, respectively) except near the surface, where they are significantly downgradient within an important region we refer to as the "surface diabatic layer" (SDL), which is analogous to the "surface layer" discussed by Treguier et al. (1997), Held and Schneider (1999), and Koh and Plumb (2004) in isopycnal or isentropic coordinate formalisms.

The equilibrium state is then reanalyzed in section 4 from a TEM perspective. As expected theoretically, the residual circulation and residual fluxes of buoyancy and of PV are very weak within the adiabatic interior: essentially all the dynamics of the problem are contained within the SDL. The residual circulation is weak—which makes this flow a special case of the range of possibilities discussed by Marshall and Radko (2003) in the context of the Antarctic Circumpolar Current—because adiabatic conditions in the interior preclude residual flow across the isopycnals and the tank geometry precludes residual mean flow along them. (The Eulerian-mean circulation, by contrast, does not vanish but is dominated by the wind-driven circulation.) The reasons for interior PV homogenization become clear in the TEM perspective as a result of the absence of a residual circulation: as found by Marshall and Radko (2003), PV must then be homogenized in the interior if the eddies transport PV downgradient, since there is no residual mean flux to balance and eddy flux. In section 4b, we use these results to reconstruct the mean buoy-

Corresponding author address: Dr. R. Alan Plumb, MIT, DEAPS, MIT Building 54, Room 1712, 77 Massachusetts Avenue, Cambridge, MA 02139.
E-mail: rap@rossby.mit.edu

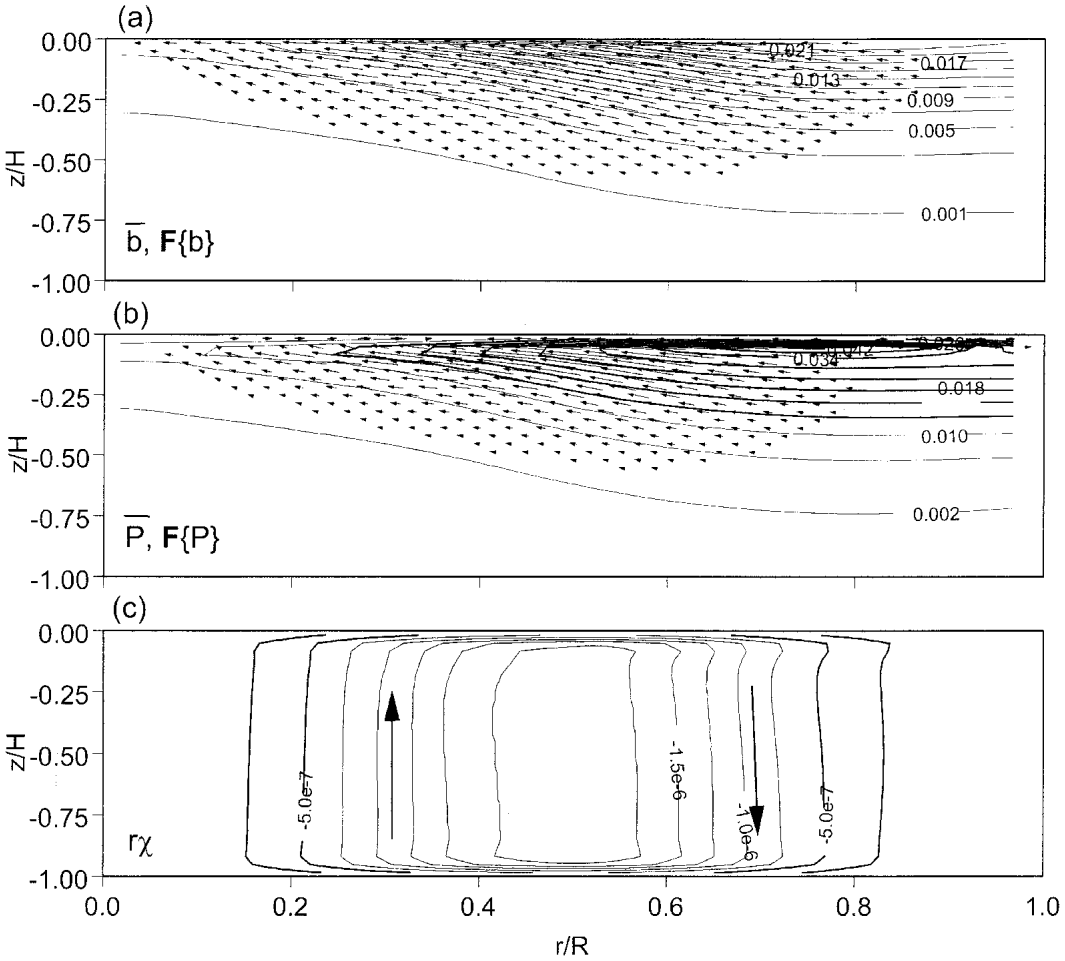

FIG. 1. Cross section of key quantities in the model equilibrium state. (a) Mean buoyancy $\overline{b}$ (m s^{-2}; contours) and eddy buoyancy flux $\overline{\mathbf{u}'b'}$ (arrows; the largest arrow corresponds to a flux 3.45×10^{-6}m^2 s^{-3}, and fluxes with magnitude less than 5% of this are not plotted). (b) Mean Ertel PV $\overline{P}$ (contours; s^{-3}) and eddy PV flux $\overline{\mathbf{u}'P'}$ (arrows; longest arrow corresponds to a flux 1.17×10^{-5}m s^{-4}, and fluxes with magnitude less than 5% of this are not plotted). (c) Volume streamfunction $r\chi$ of the meridional circulation $\overline{\mathbf{u}} = (\overline{v}, \overline{w})$. Note that $\overline{\mathbf{u}} = -\nabla \times \mathbf{j}\chi = -r^{-1}\mathbf{j} \times \nabla(r\chi)$ where $\mathbf{j}$ is the azimuthal unit vector, so the flow is along the streamlines of $r\chi$, as shown. The arrows show the sense of the circulation. Contour interval is 2.5×10^{-7} m^3 s^{-1}.

ancy structure: the only inputs required to do so (apart from the externally imposed stress and buoyancy flux) are the transfer coefficient for buoyancy within the SDL, and the effective depth (a quantity to be defined) of the SDL. The only eddy closure required in the interior is the knowledge that mean PV is homogenized along mean isopycnals.

2. Model details

The flow we consider is the same as the "reference experiment" of KJM; the geometry and imposed parameters of the numerical simulation are based on the laboratory experiment of Marshall et al. (2002). The schematic Fig. 2 of KJM shows the essential features: the fluid is contained within a cylindrical tank, with a rigid lid at $z = 0$, a flat-bottom boundary at $z = -H = -0.15$ m, with no-slip boundary conditions there and at the side walls at $r = R = 0.6$ m. The system is forced at the surface with a wind stress and a prescribed surface buoyancy flux, which are shown in Fig. 3 of KJM. The numerical model used is the "MITgcm" (Marshall et al. 1997a,b); included in the model are small-scale diffusion of momentum and buoyancy, and convective adjustment. There is no imposed mixed layer. The key parameters are given in KJM.

The model was integrated from a state of rest and uniform buoyancy. Initially, only the surface wind stress was applied. A steady Ekman flow developed, at which point the surface buoyancy forcing was switched on, producing a baroclinically unstable stratification. Eventually, the imposed forcing, in collusion with baroclinic eddies, sets up a statistically steady state. All results presented here are taken after this time; the run was

integrated for 2150 rotational periods, and results were averaged in time over the final 240 periods.

3. The equilibrium state

The azimuthal mean equations for this system are

$$\begin{aligned} \overline{m}_t + \overline{\mathbf{u}} \cdot \nabla \overline{m} &= -\nabla \cdot \mathbf{F}\{m\} + \overline{X}, \\ f\overline{m}_z &= -r\overline{b}_r, \\ \frac{1}{r}(r\overline{u})_r + \overline{w}_z &= 0, \quad \text{and} \\ \overline{b}_t + \overline{\mathbf{u}} \cdot \nabla \overline{b} &= -\nabla \cdot \mathbf{F}\{b\} - \overline{B}_z. \end{aligned} \tag{1}$$

These equations are identical to those of Part I, except for the change to cylindrical coordinates (r, θ, z), so that the overbar represents azimuthal average, $m = \frac{1}{2}fr^2 + rv$ represents the angular momentum per unit mass, $\overline{X}$ is the mean torque per unit mass, and $\overline{B}$ is the mean diabatic buoyancy flux, representing convection and small-scale diffusion, assumed to be purely vertical (the small-scale horizontal diffusion in the model makes an insignificant contribution to the mean budget). Both the mean meridional velocity $\overline{\mathbf{u}} = (\overline{u}, \overline{w})$ and eddy fluxes $\mathbf{F}\{c\} = \overline{\mathbf{u}'c'}$ are here treated as vectors in the r–z plane.

a. Structure of the equilibrium state

The equilibrium state of the model, and the eddy fluxes maintaining it, are shown in Fig. 1. The equilibrium distribution of zonal mean buoyancy $\overline{b}$ is shown in Fig. 1a, along with the vector eddy buoyancy flux $\overline{\mathbf{u}'b'}$. The stratification is confined essentially to the upper half of the domain, and the eddy flux also to the upper half, and to the central part of the channel where the wind stress and baroclinicity are greatest. One of the most striking aspects is the extent to which the buoyancy fluxes are directed along the $\overline{b}$ contours, rather than downgradient (i.e., the flux is "skew"), in the fluid interior: this is a well-known consequence of the adiabatic nature of the eddies there (e.g., Plumb 1979; Treguier et al. 1997). This is not the case, however, within a few model layers of the surface, where there is a substantial downgradient component to the eddy fluxes. (The same is also true in the bottom layers but is not evident in the figure because the buoyancy fluxes are so weak there.) This surface diabatic layer (hereinafter SDL) is the only region where the eddies effect substantial transport across isopycnals; we shall discuss this important region and its consequences in some detail below.

The distributions of mean Ertel potential vorticity $\overline{P} = \overline{\zeta_a \cdot \nabla b}$ (PV) and the eddy PV flux $\overline{\mathbf{u}'P'}$ are shown in Fig. 1b. Like the buoyancy flux, the PV flux is skew in the adiabatic interior, but not within the SDL, where it is predominantly directed downgradient, away from the PV maximum just below the surface in the outer part of the domain. A second striking aspect of the equilibrium state is the similarity of the shapes of the mean buoyancy and PV contours: $\overline{P}$ is almost homogenized along $\overline{b}$ surfaces everywhere in the adiabatic interior, though not near the surface. Given the similarity of $\overline{b}$ and $\overline{P}$ contours, note that Fig. 1b implies within the adiabatic interior a substantial eddy PV flux along the mean isopycnals.

Last, we complete the description of the equilibrium state by showing in Fig. 1c the mean meridional streamfunction χ, defined such that the meridional mean flow is

$$\overline{\mathbf{u}} = (\overline{u}, \overline{w}) = -\nabla \times (\mathbf{j}\chi) = -r^{-1}\mathbf{j} \times \nabla(r\chi), \tag{2}$$

where $\mathbf{j}$ is the unit vector in the azimuthal direction. The circulation is straightforward, with almost vertically uniform vertical mean flow supplied by Ekman pumping from the top and bottom model layers.

b. Eddy fluxes of buoyancy and PV

It is worth dwelling briefly on the form of the eddy fluxes shown in Fig. 1. As already noted, the eddy buoyancy flux is directed along the mean buoyancy contours within the interior. As is well known, this is to be expected, since

$$\overline{\mathbf{u}'b'} \cdot \nabla \overline{b} = -\overline{b'\frac{\partial B'}{\partial z}} - \left(\frac{\partial}{\partial t} + \overline{\mathbf{u}} \cdot \nabla\right)\left(\frac{1}{2}\overline{b'^2}\right) - \nabla \cdot \frac{1}{2}\overline{\mathbf{u}'b'^2}. \tag{3}$$

In a statistically steady state, then we expect the component of flux across the mean isopycnals to vanish if the eddies are locally adiabatic, and if mean meridional advection of buoyancy variance and the triple correlation term are both negligible (e.g., Plumb 1979; Treguier et al. 1997). While there is no guarantee that these terms are indeed small in our case of fully equilibrated baroclinic eddies, the empirical result that $\overline{\mathbf{u}'b'} \cdot \nabla \overline{b} \simeq 0$ in the interior is in accord with other experience (e.g., Plumb and Mahlman 1987) with zonal averages.[1]

The nonlinearities are clearly not negligible within the SDL, however. The term in (3) involving $\partial B/\partial z$ differs significantly from zero only within the top model layer, where the surface fluxes are imposed; nevertheless, we have already remarked that the downgradient component of the buoyancy flux is manifestly nonzero in a few layers below the top, which must imply that the remaining terms in (3) are playing a role. In the absence of a mixed layer (as is the case in our simulation), the SDL corresponds to the surface zone discussed by Held and Schneider (1999) and Koh and Plumb (2004), as the region spanned by those (three dimensional) isopycnals

[1] McDougall and McIntosh (1996) have shown how this argument can be refined in the nonzonally averaged case where there may be large mean advection of buoyancy variance.

that are ventilated at some azimuth (or time). When averaging in isopycnal coordinates, diabatic effects—through the surface buoyancy flux—enter the averages directly, throughout this region. In our z-coordinate case (unlike the isopycnally averaged problem), the diabatic buoyancy flux enters the average in (3) only in the topmost model layer where $\partial B/\partial z$ is nonzero:[2] information that the isopycnals outcrop at some azimuth is carried into the average only through the remaining terms in (3). In the absence of a mixed layer, the maximum thickness δ of the ventilated layer—and thus our estimate of the thickness of the surface zone—is

$$\delta \sim \delta_b = \overline{b}_z^{-1}(\overline{b'^2})^{1/2}, \tag{4}$$

where $\sqrt{\overline{b'^2}}$ is the eddy buoyancy perturbation at the surface and $\overline{b}_z$ the mean gradient within the SDL. We shall in fact introduce a somewhat different measure of the depth of the SDL in section 4b(3).

Much the same could be said for the PV fluxes as for the buoyancy fluxes: they obey an equation analogous to (3) and therefore are expected to be, and in practice are, directed along the $\overline{P}$ (and $\overline{b}$) contours in the adiabatic, inviscid interior where PV is conserved, but not within the SDL. The fact that the eddy PV flux along the mean isopycnals is nonzero in the interior, while the mean gradient of PV along the mean isopycnals is essentially zero, is significant, since it shows that any attempt to represent this component of the flux in the form

$$\overline{v'P'}|_{\overline{b}} = -K\,\nabla\overline{P}|_{\overline{b}} \tag{5}$$

is doomed to fail, since it would predict no flux.[3] As discussed at length in Part I, this does not mean that the approach itself is doomed, but that the expression on the left of (5) is not the only, nor in fact the most appropriate, definition of eddy flux. (It is clearly not the same thing, for example, as the isopycnal component of the isopycnal-mean flux.)

c. *Momentum, buoyancy, and PV balances: Conventional analysis*

Diagnostically, the key balances in the equilibrated state of the modeled flow are simple to describe. Given that (i) the direct contribution of diffusion to the angular momentum budget is negligible outside the Ekman layers, so $\overline{X} = r\tau_z$, where τ is the zonal stress on a horizontal surface (so $\overline{X} = 0$ in the interior); (ii) that the term $\overline{\mathbf{u}} \cdot \nabla\overline{m}$ is dominated by the Coriolis term $r\overline{u}f$; and (iii) that the eddy angular momentum fluxes play a very minor role, the steady angular momentum budget is, from the first of (1),

$$\frac{1}{r}\,\overline{\mathbf{u}} \cdot \nabla\overline{m} \simeq f\overline{u} = \tau_z. \tag{6}$$

Hence the radial component of the mean circulation must vanish outside the Ekman layers, as is evident from Fig. 1c. [The slight deviation of the streamlines just below the surface in the outer part of the channel is because of a small contribution there of the Reynold's stress term, $-r^{-1}(r\overline{u'm'})_r$.] Equation (6) integrates, using (2) and given $\chi = 0$ at the surface, to

$$\chi = -\frac{\tau_s}{f}, \tag{7}$$

where τ_s is the surface wind stress. Given that the eddy fluxes of angular momentum are largely negligible, the overall angular momentum balance is as depicted schematically in the upper frame of Fig. 2: angular momentum is input at the surface by the wind stress, carried directly downward by the meridional circulation, and extracted by the stress at the bottom boundary.

In the adiabatic interior, the steady buoyancy budget is simply a balance between mean advection and the eddy flux divergence. Given that the radial mean velocity $\overline{u}$ is essentially zero in the interior and that, for small Rossby number as is appropriate to our example, the eddy flux divergence is dominated by the horizontal term, this balance is

$$\overline{w}\overline{b}_z = -\frac{1}{r}\,(r\overline{u'b'})_r. \tag{8}$$

This balance—first discussed by Gill et al. (1974)—was at the heart of the discussions in Johnson and Bryden (1989), KJM, and Marshall et al. (2002) on the role of eddies in setting ocean stratification. If $\overline{w}$ is controlled by the wind stress, the interior stratification of the equilibrium state exists only by virtue of the eddy transport. Within the SDL, the balance is more complex, with the mean circulation, eddy transport, and surface buoyancy fluxes all playing a role, as depicted in the lower frame of Fig. 2.

4. The equilibrium: TEM analysis

The TEM equations for this system are

$$\begin{aligned} \overline{m}_t + \overline{\mathbf{u}}^\dagger \cdot \nabla\overline{m} &= -\nabla \cdot \mathbf{F}^\dagger\{m\} + \overline{X}, \\ f\overline{m}_z &= -r\overline{b}_r, \\ \frac{1}{r}\,(r\overline{u}^\dagger)_r + \overline{w}^\dagger_z &= 0, \quad \text{and} \\ \overline{b}_t + \overline{\mathbf{u}}^\dagger \cdot \nabla\overline{b} &= -\nabla \cdot \mathbf{F}^\dagger\{b\} - \overline{B}_z. \end{aligned} \tag{9}$$

As discussed in Part I,

$$\overline{\mathbf{u}}^\dagger = \overline{\mathbf{u}} + \nabla \times \mathbf{j}\psi \tag{10}$$

(where $\mathbf{j}$ is the azimuthal unit vector) is the residual mean circulation and

[2] In the inner part of the cylinder where the surface buoyancy is low, convection also plays a role below the topmost layer.

[3] Of course, the mean PV gradient along mean isopycnals is not exactly zero, but it is weak and of inconsistent sign.

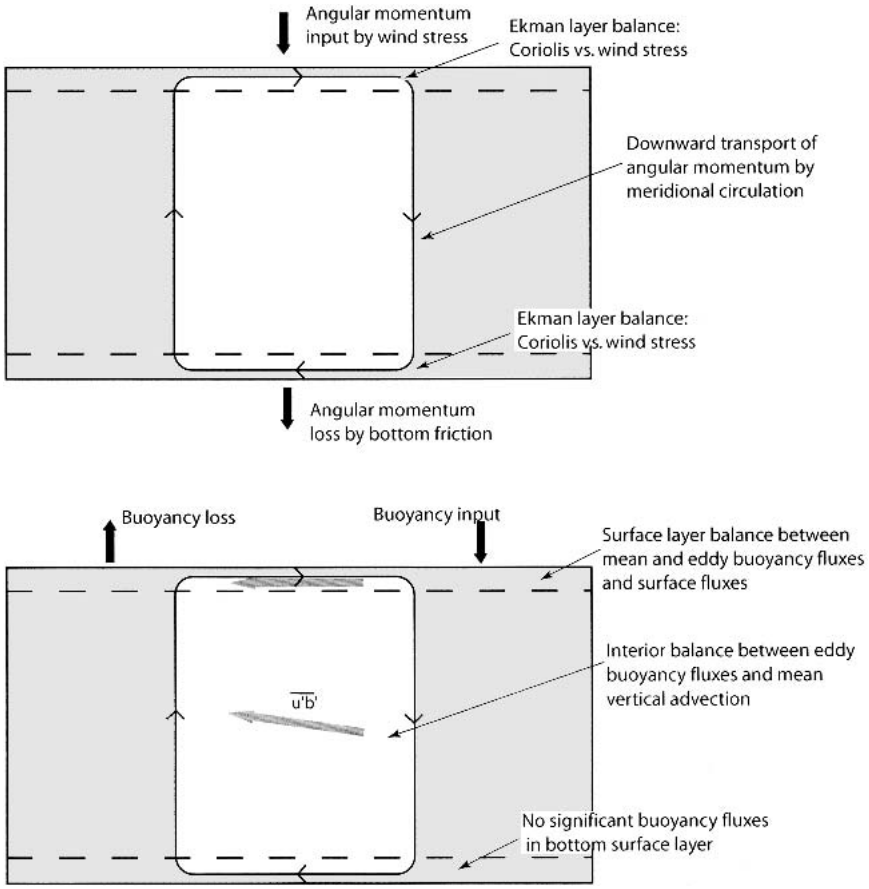

FIG. 2. A schematic depiction of the conventional momentum and buoyancy budgets. See text for discussion.

$$\mathbf{F}^{\dagger}\{c\} = \mathbf{F}\{c\} - \psi \mathbf{j} \times \nabla \bar{c} \tag{11}$$

is the residual eddy flux of c. Following Part I, we adopt the coordinate-independent definition

$$\psi = -|\nabla \bar{b}|^{-1} \boldsymbol{\tau}\mathbf{s} \cdot \overline{\mathbf{u}'b'}, \tag{12}$$

where $\mathbf{s} = \mathbf{j} \times \nabla \bar{b}/|\nabla \bar{b}|$ is the outward unit vector along the mean isopycnals, for the quasi-Stokes streamfunction. Note that (9)–(12) are the equations used by Marshall and Radko (2003) in their residual mean model of the ACC, except that they used the Held and Schneider (1999) definition of ψ, rather than (12).

The theoretical impact of using different definitions of ψ is discussed at some length in Part I, in which it is argued that the form (12) has a number of advantages. One of these is that, in the presence of a mixed layer, $\mathbf{s}$ becomes normal to a horizontal upper surface and consequently ψ and the normal component of $\bar{\mathbf{u}}^{\dagger}$ vanish there, thus guaranteeing (unlike the quasigeostrophic definition $\psi = -\overline{u'b'}/\bar{b}_z$) no residual mean flow through the boundary. In the present case, where there is no mixed layer, we simply impose at the top of the model one of vanishing thickness, and with horizontal velocities and buoyancy equal to the values immediately below this layer. Thus, in the following discussion, the upper surface is taken to be immediately above this thin added mixed layer.

a. Residual circulation and fluxes

The equilibrium state of the model, viewed from the transformed Eulerian-mean perspective, is depicted in Fig. 3. The residual circulation (lowest frame) has almost vanished in the interior: in the residual picture, the circulation is essentially confined to the surface diabatic layers near the top (and, to a lesser extent, bottom) boundary. The overturning circulation, as measured by the maximum value of streamfunction in the interior, is reduced by a factor of more than 90% compared with the Eulerian circulation, reflecting the high degree of cancellation between the Eulerian-mean and quasi-Stokes velocities. (The cancellation is more complete than in KJM, a result of our different way of calculating the residual velocity.) The residual fluxes of buoyancy and of PV are shown in the two upper frames.

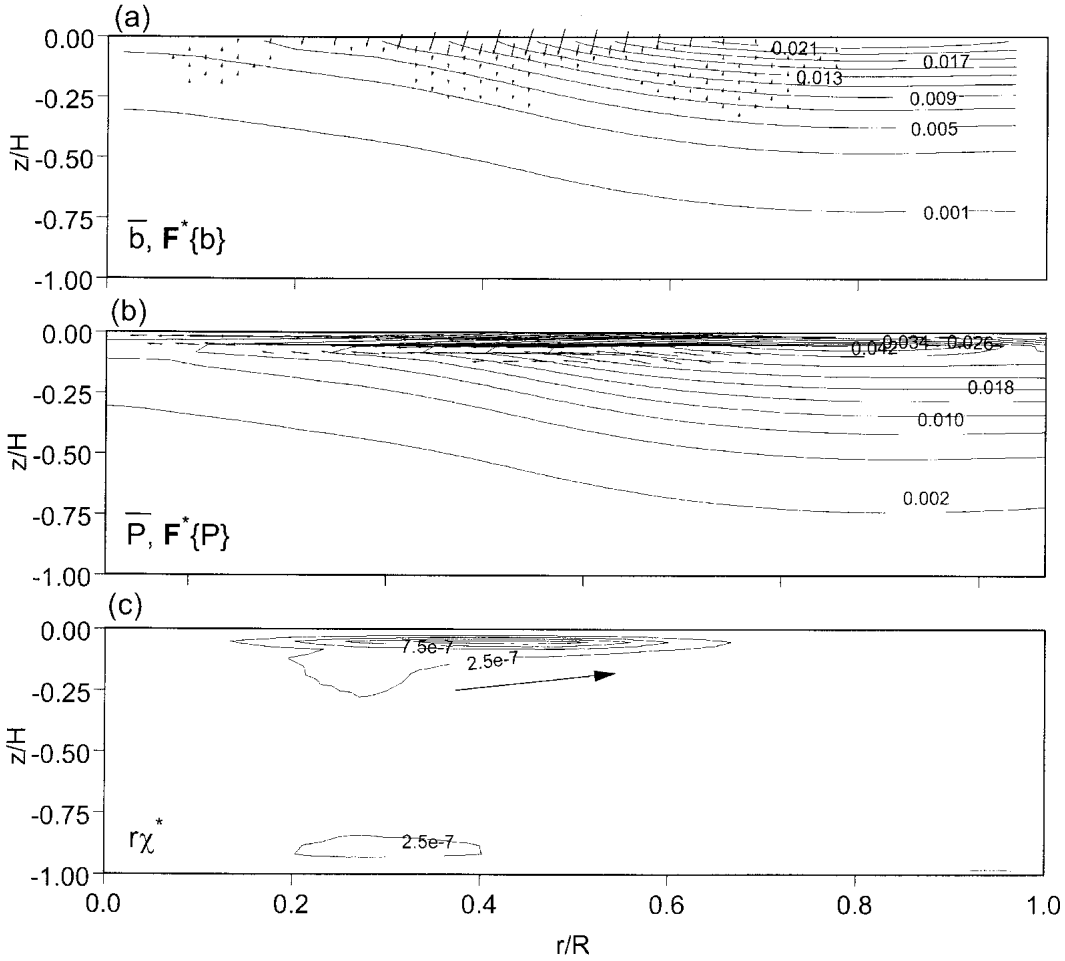

FIG. 3. Cross section of key quantities in the TEM analysis of the model equilibrium state. (a) Mean buoyancy $\overline{b}$ (m s^{-2}; contours) and residual eddy buoyancy flux $\mathbf{F}^{\dagger}\{b\}$ (gridpoint-centered arrows; the scale is the same as in Fig. 1a). Note that the normal component of this flux vanishes at the surface: those arrows that appear to penetrate the surface refer to the first layer below the surface. (b) Mean Ertel PV $\overline{P}$ (contours; s^{-3}) and residual eddy PV flux $\mathbf{F}^{\dagger}\{P\}$ (arrows; same scale as Fig. 1b). (c) Volume residual streamfunction $r\chi^{\dagger}$ of the meridional circulation. The contour interval is 2.5×10^{-7} m^3 s^{-1}. The arrow in (c) shows the sense of the residual circulation.

As anticipated, the dominant skew components of the fluxes within the adiabatic interior have been removed by the transformation, leaving significant fluxes of buoyancy and PV only within the SDL, where the fluxes of both are predominantly downgradient.

While the vanishing of the skew component of the residual eddy flux of buoyancy is guaranteed by the definition of the quasi-Stokes streamfunction (12), the fact that the same is true of the residual eddy PV flux (as evident in Fig. 3b) indicates that the effective advecting velocity that produces the skew fluxes is the same for both quantities. In terms the discussion in section 7 of Part I, this amounts to asserting that the ratio

$$\sigma = \left(\frac{\mathbf{s} \cdot \overline{\mathbf{u}'b'}}{|\nabla \overline{b}|} \right)^{-1} \frac{\mathbf{s}_P \cdot \overline{\mathbf{u}'P'}}{|\nabla \overline{P}|}, \tag{13}$$

where $\mathbf{s}_P$ is the unit vector along the PV contours, be equal to unity, in which case the skew fluxes of buoyancy and of PV are in the same proportion as their mean gradients. Except in the surface layer, and near the sides and bottom of the domain where the fluxes are small and the ratio is ill defined, σ is within 10% of unity. As is evident from (18) of Part I, the skew component of the residual eddy PV flux, $\mathbf{s}_P \cdot \mathbf{F}^{\dagger}\{P\}$, vanishes if $\sigma = 1$.

We also show, in Fig. 4, the residual eddy angular momentum flux $\mathbf{F}^{\dagger}\{m\}$. The flux is dominated by the vertical component $-fr\psi$, though with significant contribution from the horizontal Reynolds' stress $\overline{ru'v'}$ near the surface. As we shall see in section 4b(1), the vertical independence of the flux in the interior is a consequence of the fact that the role of $\mathbf{F}^{\dagger}\{m\}$ is to communicate the surface wind stress down to the bottom of the fluid. The role of the Reynolds stresses in

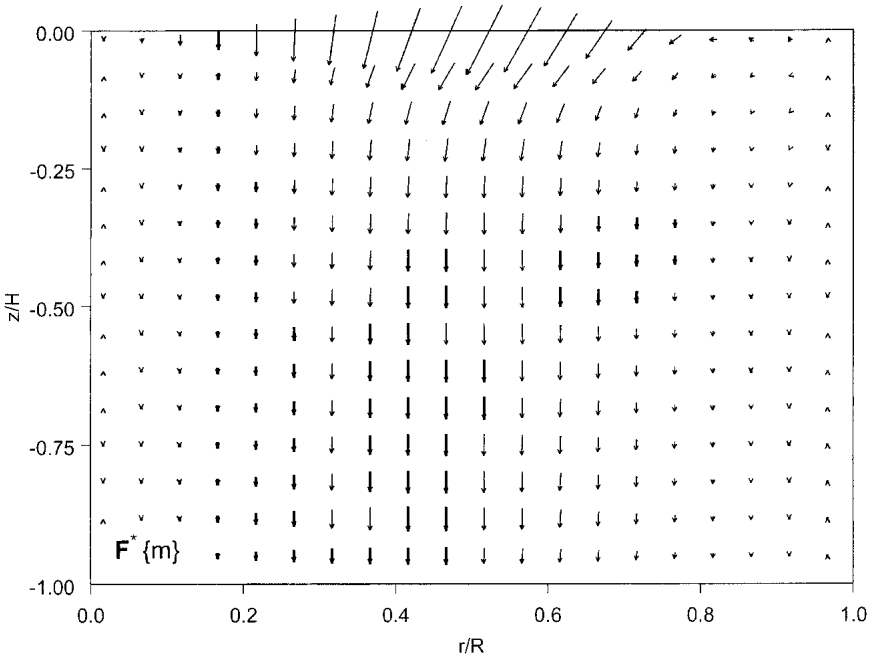

FIG. 4. The residual angular momentum flux $\mathbf{F}^{\dagger}\{m\}$. Just as in Fig. 3a, the vertical component vanishes at the surface; those vectors appearing to penetrate the surface refer to locations just below the surface.

this case is to direct the net stress slightly toward the center of the tank (so that the stress on the bottom reflects the wind stress at slightly larger radius).

Overall, the TEM budgets are depicted schematically in Fig. 5. To a good approximation, the TEM angular momentum balance is, as just stated and as described by Johnson and Bryden (1989), simply a matter of the eddies transferring the imposed wind stress downward. This contrasts with the conventional-mean view, shown in Fig. 2, of momentum transfer by the Ekman-driven meridional circulation. The TEM buoyancy budget is similarly straightforward: transport is negligible in the adiabatic interior, and so all the fluxes required to transport buoyancy from the region (at large r) of surface buoyancy input to the region of loss at small r occur within the SDL. Both the residual eddy fluxes and advection by the residual circulation, recirculating within the SDL, play a role in this transport.

b. Analysis of the TEM balances

1) INTERIOR BUOYANCY BUDGET

If diabatic processes are negligible in the interior, then $\mathbf{F}^{\dagger}\{b\} = 0$ (Treguier et al. 1997), and so the TEM buoyancy budget becomes, in adiabatic steady state,

$$\overline{\mathbf{u}}^{\dagger} \cdot \nabla b = 0 \tag{14}$$

in the interior: the residual flow must be confined to buoyancy surfaces. In fact, mass continuity then requires that the volume flux between two adjacent mean isopycnals be spatially uniform—that is, $\mathbf{s} \cdot \overline{\mathbf{u}}^{\dagger} |\nabla \overline{b}|^{-1}$ is constant along mean isopycnals, where $\mathbf{s} \cdot \overline{\mathbf{u}}^{\dagger}$ is the component of the residual velocity along the mean isopycnals. However, since all isopycnals (except a few near the surface maximum) are laterally bounded, outcropping into the SDL only at the inner end and not entering the bottom layer (Fig. 1a), it follows that $\overline{\mathbf{u}}^{\dagger} = 0$ and hence

$$\chi^{\dagger} = 0 \tag{15}$$

throughout the interior, consistent with Fig. 3c. Hence, from (7) and (10), with (12),

$$-\psi = \frac{\overline{\mathbf{u}'b'} \cdot \mathbf{s}}{|\nabla \overline{b}|} = \frac{\tau_s}{f} \tag{16}$$

there, expressing the balance between wind-driven steepening of the isopycnals and the flattening by eddy fluxes (cf. KJM), a statement almost identical to (8). It is this balance that shows up in the vertical coherence of the residual eddy angular momentum flux in Fig. 4, since $F^{\dagger(z)}\{m\} \simeq -fr\psi = r\tau_s$.

2) INTERIOR MOMENTUM BALANCE

Neglecting small-scale friction in the interior and using $\mathbf{F}^{\dagger}\{b\} = 0$ there, the steady transformed angular momentum budget for Ro $\ll 1$ is, from the first of (9) and from (26) of Part I,

$$f|\nabla \overline{b}|\,\overline{u}^{\dagger} = \mathbf{s} \cdot \mathbf{F}^{\dagger}\{P\}, \tag{17}$$

where $\mathbf{s}_P \cdot \mathbf{F}^{\dagger}\{P\}$ is the component of the residual eddy flux of Ertel PV along the mean isopycnals. In general,

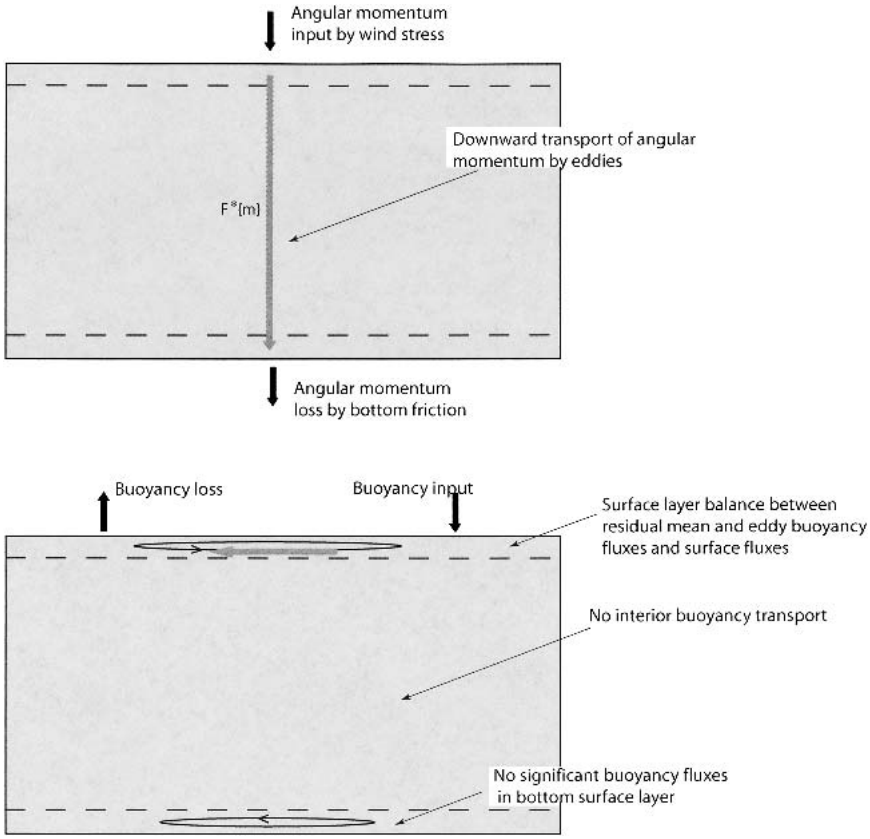

FIG. 5. Schematic of the transformed budgets of (top) angular momentum and (bottom) buoyancy. See text for discussion.

(17) expresses a balance between residual mean and eddy fluxes of PV. As we have just seen from (15), the residual mean advection vanishes in this case and it then follows that

$$\mathbf{s} \cdot \mathbf{F}^{\dagger}\{P\} = 0 \tag{18}$$

in the interior, since there is nothing in the equilibrated state to balance eddy PV transport. The empirical fact that $\mathbf{s} \cdot \nabla \overline{P} = 0$ in the interior, together with (18), is evidence that, in the presence of eddy stirring, one way (perhaps the only way) of achieving zero flux is to eliminate the mean gradient. To put the same thing another way, in the absence of residual mean advection or any other process that might restore a mean gradient, the eddies stir any preexisting gradient into oblivion.

3) SDL BUOYANCY BUDGET

Near the surface layer, there is a nonzero residual mean flow, recirculating within the SDL, and a nonzero residual eddy buoyancy flux. Since vertical diffusion dominates over small-scale horizontal diffusion near the surface, we may write the mean buoyancy budget there as

$$\frac{\partial \overline{b}}{\partial t} + \overline{\mathbf{u}}^{\dagger} \cdot \nabla \overline{b} = -\nabla \cdot \mathbf{F}^{\dagger}\{b\} - \overline{B}_z.$$

At the bottom of the surface layer, the eddies are adiabatic and so $\mathbf{F}^{\dagger}\{b\} = 0$ and $\chi^{\dagger} = 0$ there. At the top of the layer (which is the top of the thin, introduced mixed layer), the normal component of $\mathbf{F}^{\dagger}\{b\}$ at the surface is also zero, as is $\chi^{\dagger}$. If we integrate from any point z_i within the adiabatic interior, the integrated steady balance is

$$\int_{z_i}^{z_S} \nabla \cdot (\chi^{\dagger} \mathbf{j} \times \nabla \overline{b})\, dz + \int_{z_i}^{z_S} \nabla \cdot \mathbf{F}^{\dagger}\{b\}\, dz = -\overline{B}_S,$$

where $\overline{B}_S$ is the surface value (defined positive upward). There is no contribution to the integrals from within the interior. Applying the conditions at top and bottom of the surface layer, we have

$$\frac{1}{r}\frac{\partial}{\partial r}\left[r \int_{z_i}^{z_S} (F^{\dagger(r)}\{b\} + \chi^{\dagger}\overline{b}_z)\, dz \right] = -\overline{B}_S. \tag{19}$$

The surface buoyancy structure is thus simply determined by a balance between the net horizontal buoyancy transport within the surface diabatic layer, and surface buoyancy fluxes. No other effects come into

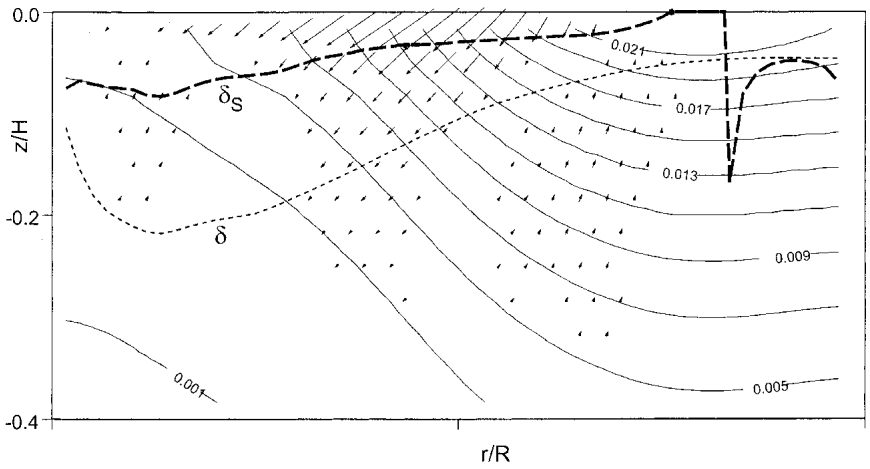

FIG. 6. The thickesses δ and δ_S of the SDL (the thin, short-dash curve shows $z = -\delta$; the heavy, long-dashed curve shows $z = -\delta_S$), superimposed on the mean buoyancy (contours, m s^{-2}) and residual buoyancy flux $\mathbf{F}^{\dagger}\{b\}$. Note that only the upper part of the domain is shown.

play because both the residual circulation and the residual buoyancy flux vanish below the surface layer, and so there is no transport of buoyancy into or out of the base of the layer. This fact makes (19) subtly different from the balance discussed by Marshall (1997); the residual circulation, which here simply recirculates within the SDL, plays a role in the surface heat budget only by virtue of the nonvanishing of $\overline{b}_z$ within the SDL.[4] Therefore, the contribution of residual mean advection to the integrated SDL buoyancy (19) is smaller than a straightforward scaling analysis [such as that of Treguier et al. (1997)] might suggest, and while the mean component is not negligible, the residual eddy flux is in this case the dominant term in the surface layer buoyancy budget.

Now, $\chi^{\dagger}$ vanishes at the surface and below the SDL; assuming that the SDL is thin, with little variation of eddy buoyancy flux in the vertical direction, the typical magnitude of the term $|\chi^{\dagger}\partial\overline{b}/\partial z| \lesssim |\overline{u'b'}_s|$, the surface eddy buoyancy flux. Since $F^{\dagger(r)}\{b\}$ has a magnitude $|\overline{u'b'}_s|$ at z_s and vanishes in the interior, the entire integrand in (19) has the same typical magnitude. Accordingly, we may define a characteristic *effective* depth, δ_S, of the SDL according to

$$\int_{z_i}^{z_S} (F^{\dagger(r)}\{b\} + \chi^{\dagger}\,\overline{b}_z)\,dz = \delta_S \overline{u'b'}_S. \tag{20}$$

(Note that the integral is insensitive of the value of z_i, as long as it lies below the SDL, since the integrand vanishes in the interior.) The depth δ_S, thus defined, and δ_b given by (4) are plotted in Fig. 6. The SDL, by definition (20), is quite shallow: shallower, in fact, than the estimate from (4) by a factor of 2–3, and clearly shallower than the depth over which the diabatic buoyancy fluxes are significant, as is evident on the figure. From the definition (20) we get, not a direct estimate of the actual depth of the SDL, but a more useful measure of its *effective* depth: buoyancy is transported horizontally within the SDL as if it were a layer of depth δ_S within which the total buoyancy flux is given by the surface value of $\overline{u'b'}$. In fact, from (20) and (19), the SDL buoyancy budget becomes simply

$$\frac{1}{r}\frac{\partial}{\partial r}(r\delta_S\,\overline{u'b'}_S) = -\overline{B}_S. \tag{21}$$

If we further assume that the isopycnal slope is shallow below the surface diabatic layer, and that the layer is so thin that buoyancy fluxes vary little across it[5] then, using (16),

$$\overline{u'b'}_S \simeq \overline{u'b'}_B \simeq (\overline{b}_z)_B\,\frac{\tau_s}{f}, \tag{22}$$

where the subscript B denotes the value at the base of the SDL. Making this substitution in (20) and (19), we achieve an expression for the stratification at the base of the SDL:

$$(\overline{b}_z)_B = -\frac{f}{\tau_s\delta_S}\int_0^r r\overline{B}_S\,dr, \tag{23}$$

where we have assumed $\overline{b}_z = 0$ at $r = 0$, where convection sets the stratification. No formal closure assumption has been made to this point. Note that (23) expresses the eddy-determined stratification at the base of the surface layer in terms of the surface buoyancy input and wind stress, and does not include any explicit

[4] This would still be true in the presence of a mixed layer, since then the SDL would then be deeper than the mean mixed layer.

[5] The buoyancy flux actually decreases by about 20% from top to bottom of the SDL.

eddy flux terms (though it does involve the thickness δ_S, which will be sensitive to eddy amplitude). The eddy buoyancy fluxes do not appear, simply because they must balance both the wind-driven advection (16) and the surface buoyancy input (21) and have thus been eliminated.

c. Reconstruction of the equilibrium state

To go further, we need to make a closure assumption for the surface buoyancy fluxes. Since there is no vertical motion there, there is no skew flux: transport is locally two-dimensional, and it is reasonable to expect a flux–gradient parameterization of the form

$$\overline{u'b'}_S = -K\frac{\partial \overline{b}_S}{\partial r} \tag{24}$$

to be useful. The actual relationship between the surface flux and mean gradient of buoyancy is shown in Fig. 7. The linearity of this relationship through most of the domain is remarkable and implies a constant value of $K = 4.8 \times 10^{-5}$ m^2 s^{-1}. This is convenient, if a little surprising [there is no reason why K in (24) should not be a function of r]. The linearity breaks down in the outer part of the domain where $\partial \overline{b}_S/\partial r$ changes sign. Given (24), (21) becomes simply

$$\frac{1}{r}\frac{\partial}{\partial r}\left(rK\delta_S\frac{\partial \overline{b}_S}{\partial r}\right) = \overline{B}_S, \tag{25}$$

from which the surface distribution of mean buoyancy can be determined, given $\overline{B}_S$, K, and δ_S.

Using (24) and the assumption of a thin SDL, we have from (22),

$$\overline{u'b'}_B \simeq \overline{u'b'}_S = -K\frac{\partial \overline{b}_S}{\partial r} \simeq -K\left(\frac{\partial \overline{b}}{\partial r}\right)_B = \frac{1}{f}\tau_S\left(\frac{\partial b}{\partial z}\right)_B,$$

so that, at the base of the layer, the isopycnal slope is just

$$\gamma_B = -\left(\frac{\partial b/\partial r}{\partial b/\partial z}\right)_B \simeq -\frac{\tau_S}{fK}, \tag{26}$$

and the stratification is

$$\left(\frac{\partial b}{\partial z}\right)_B = -\frac{fK}{\tau_S}\frac{\partial \overline{b}_S}{\partial r}, \tag{27}$$

from which we can determine the PV there. Marshall and Radko (2003) followed the same approach in their analysis of the Antarctic Circumpolar Current, though with more generality (they also investigated cases with nonzero residual mean circulation), and they parameterized K in terms of the mean isopycnal slope, which we make no attempt to do in this diagnostic study.

We could now construct the full solution, using (25) to determine $\overline{b}_S(r)$, and (26) to determine the isopycnal slope at the base of the surface diabatic layer. To do so, we require the externally imposed surface buoyancy flux B_S and the wind stress (both of which of course we know), together with the surface diffusivity K and the surface diabatic layer thickness δ_S. In fact, the only other input needed to complete the mean buoyancy field everywhere is the knowledge that PV is homogenized along mean isopycnals in the interior, since for

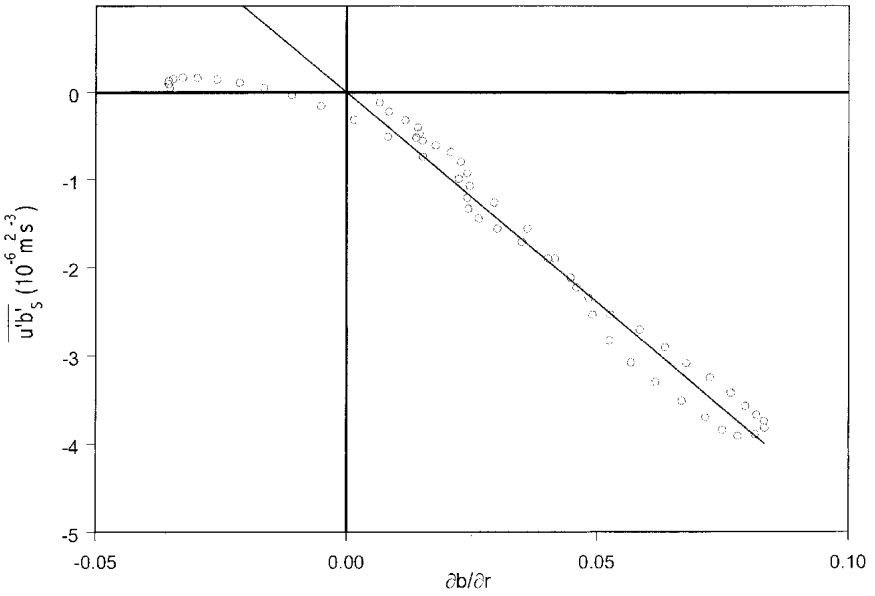

FIG. 7. The surface buoyancy flux $\overline{u'b'}_s$ vs the surface mean buoyancy gradient $\overline{b}_r$. Each point is a grid point along the surface: those points with negative mean gradient are in the outer part of the domain (cf. Fig. 3a). The superimposed line has slope -4.8×10^{-5} m^2 s^{-1}.

$\overline{P} \simeq f\overline{b}_z$ (a good approximation here) this implies that the isopycnal slope is independent of z throughout the interior. There is no need to parameterize either buoyancy fluxes or PV fluxes in the interior.

Results of this reconstruction, using the constant values $K = 4.8 \times 10^{-5}$ m^2 s^{-1} and $\delta_S = 0.05H = 0.0075$ m, are shown in Fig. 8. The shapes of the modeled and reconstructed isopycnals match very well, except near the buoyancy maximum in the outer part of the upper layers, where the surface flux–gradient relationship, with the chosen value of K, is not accurate. The slight mismatch in isopycnal slopes just below the surface stems from the neglect of variations in eddy buoyancy flux across the surface diabatic layer that was used to derive (22). The other significant discrepancy is an offset of the absolute values. Our reconstruction implicitly set the zero point as the deep water buoyancy and assumed that this is the same as the lowest buoyancy at the surface (at $r = 0$). In reality, we expect that convection will set the deep water buoyancy to be that of the lowest value at the surface including the eddy contribution, and therefore the *mean* surface buoyancy at $r = 0$ will be greater than that at depth by an amount corresponding to the local eddy buoyancy perturbation. While this value could be added to the input information for the reconstruction, we would need a theory for the stratification between the (few) mean isopycnals that do not outcrop in order to complete the equilibrium solution.

5. Conclusions

From a theoretical point of view, one key result of this paper, following the theoretical treatment of Part I, is the illustration in practice of the crucial distinction between "residual" eddy fluxes, and the "raw" fluxes. For example the PV flux $\overline{\mathbf{u}'P'}$ (in these z coordinates) does not vanish even when, as we found here, the mean PV gradient along the mean isopycnals vanishes, because of a presence of a large "skew" component. In contrast, the residual eddy PV flux does vanish under these circumstances. Among other things, this confirms the conclusion of Part I that, in any parameterization scheme that is centered on the eddy flux of (Ertel) PV, it is the residual eddy flux that is consistent with a flux–gradient formalism.

In the cylinder flow analyzed here, the transformed Eulerian-mean analysis allowed a simple exposition of the controlling factors in setting the equilibrium state. In the adiabatic interior, the residual circulation vanishes: the adiabaticity guarantees that there can be no residual flow across the mean isopycnals, and the blocking effects of the sidewalls prevent any flow along them.

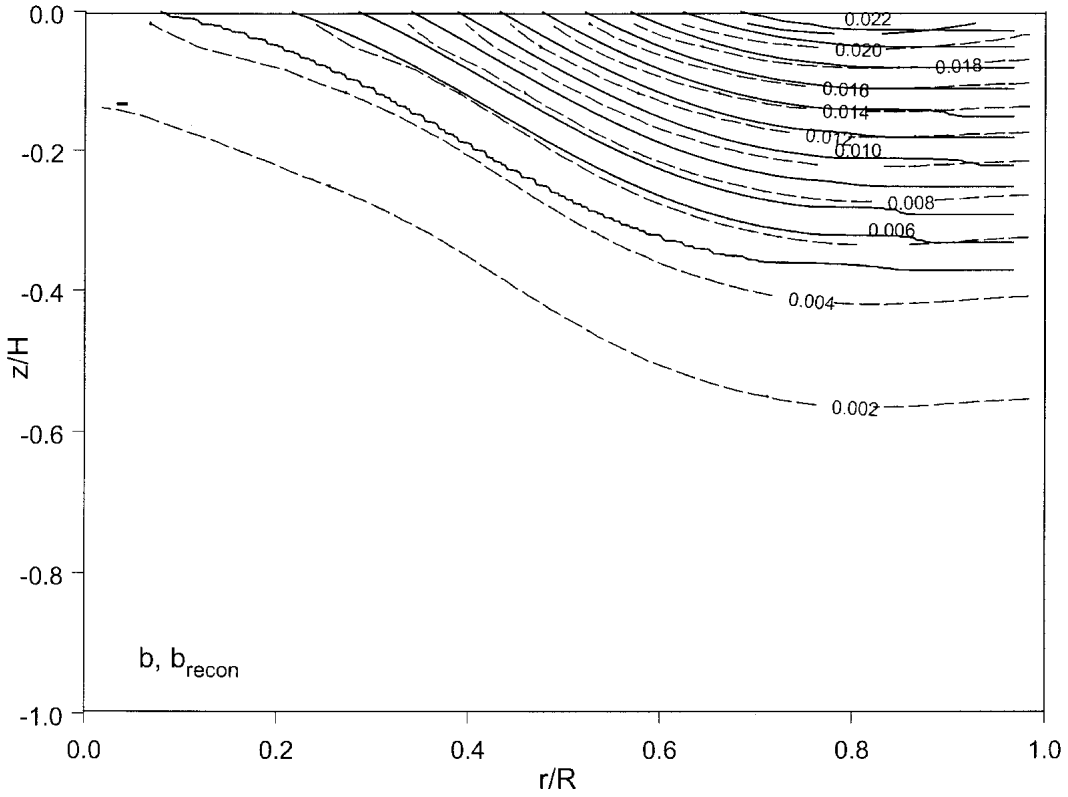

FIG. 8. Mean buoyancy contours (dashed) and reconstructed (solid) by the method outlined in section 4c. Contours values are multiples of 0.002 m s^{-2}. See text for details.

In turn, the transformed angular momentum balance makes it clear why PV must be homogenized: since there is no mean residual advection, there is nothing to oppose eddy stirring in the interior, with the consequence that PV is homogenized along the isopycnals, a scenario similar to that discussed by Rhines and Young (1982). Thus, as suggested by Treguier et al. (1997), the equilibrium state is not sensitive to the eddy mixing rate in the interior, not because the mixing is weak but, on the contrary, because it is so dominant that PV is homogenized, independent of the mixing rate.

Another consequence of the vanishing of the interior residual circulation and the consequent confinement of the residual circulation to the SDL is that there is no buoyancy advection into or out of the SDL, so that the surface buoyancy structure is simply a balance between fluxes through the surface and buoyancy transport (through the diabatic eddy fluxes and, to a lesser degree, internal residual advection) within the SDL. It is therefore these SDL fluxes that allow an equilibrium with nonzero buoyancy fluxes through the surface even though there is no residual mean advection into or out of the SDL. The scenario described here is a special case—the vanishing residual mean circulation being a consequence of the restrictive geometry—of the range discussed by Marshall and Radko (2003), with some minor modifications in the SDL buoyancy budget to allow for the residual circulation within the SDL.

It is worth noting here the potential for remote impact on the surface buoyancy budget that this chain of factors implies. The fact that, in this example, the residual circulation must recirculate within the SDL has nothing to do with the dynamics of the SDL itself, but arises because there are no diabatic effects elsewhere that could permit a return flow across the mean isopycnals. If, on the other hand, the outer walls permitted a nonzero residual flow (e.g., because of vertical mixing immediately outside the walls, or coupling to a remote ocean with significant diapycnal transport), then there appears to be nothing to preclude a residual flow of the kind discussed by Marshall and Radko (2003), with a residual circulation along the mean isopycnals in the adiabatic interior, recirculating through the SDL. The presence of such a circulation would change many things: PV would no longer be homogenized along isopycnals, since there would now be a mean residual advection of PV in addition to eddy stirring, and the surface buoyancy budget would be affected by residual mean advection into and out of the SDL. Thus, remote diabatic effects, here subsumed as the boundary condition at the outer wall, could impact the local budgets both at the surface and in the interior.

The recognition of the SDL/adiabatic interior structure of the flow allowed a straightforward analysis of the equilibrated buoyancy structure. The only inputs required for the reconstruction of the mean state were the SDL buoyancy budget (for which it was necessary to specify the horizontal diffusivity within the SDL and its depth, together with the imposed flux through the surface, yielding the surface buoyancy distribution), the vanishing of residual circulation within the adiabatic interior (which led to balance between the wind stress and the buoyancy flux, yielding the isopycnal slope immediately below the SDL), and the homogenization of PV in the interior (allowing the mean isopycnals to be constructed throughout the interior). In fact, the most important result—the slope of the isopycnals, which leads to the thermocline depth, obtained here as (26)—is identical to that derived by KJM. However, the assumptions required here are less restrictive than those used by KJM. In particular, it was not necessary to take the logically inconsistent step of using a downgradient flux–gradient relationship to represent the skew fluxes of buoyancy in the interior. It was necessary to introduce here the concept of PV homogenization, but in a less restrictive way than in KJM, who imposed an exponential vertical structure of mean buoyancy (which is in fact equivalent to assuming $\overline{P}$ to be a linear function of $\overline{b}$). Note that we made no use here of the SDL angular momentum budget, which allows determination of the structure of the residual circulation (which is confined to the SDL), since this result was not of primary interest.

Of course, the simplicity of this analysis is a consequence of the simplicity of the system under consideration. The most obvious factor is the two-dimensionality of the mean state, which by itself precludes direct application of the results to much of the ocean. Even in the case of the ACC, the situation may be more complicated: if interior or remote diabatic effects permit a nonzero residual circulation then, as already noted, mean PV may no longer be homogenized along mean isopycnals since there is then a requirement, even in the adiabatic interior, for a nonzero residual eddy PV flux to balance mean advection. In that case, the PV structure in the interior would be sensitive to eddy mixing rates within the interior.

Acknowledgments. We thank Helen Jones for advice on performing the numerical experiments, Will Heres for assistance with data analysis, and Ivana Cerovečki and Raffaele Ferrari for discussions. This work was supported by the National Science Foundation through Grant OCE-0095595.

REFERENCES

Gill, A. E., J. S. A. Green, and A. J. Simmons, 1974: Energy partition in the large-scale ocean circulation and the production of mid-ocean eddies. *Deep-Sea Res.,* **21,** 499–528.

Held, I. M., and T. Schneider, 1999: The surface branch of the zonally averaged mass transport circulation in the troposphere. *J. Atmos. Sci.,* **56,** 1688–1697.

Johnson, G. C., and H. L. Bryden, 1989: On the size of the Antarctic Circumpolar Current. *Deep-Sea Res.,* **36,** 39–53.

Karsten, R., H. Jones, and J. Marshall, 2002: The role of eddy transfer in setting the stratification and transport of a circumpolar current. *J. Phys. Oceanogr.,* **32,** 39–54.

Koh, T. Y., and R. A. Plumb, 2004: Isentropic zonal average formalism and near-surface circulation. *Quart. J. Roy. Meteor. Soc.,* **130,** 1631–1653.

Marshall, D., 1997: Subduction of water masses in an eddying ocean. *J. Mar. Res.,* **55,** 201–222.

Marshall, J., and T. Radko, 2003: Residual-mean solutions for the Antarctic Circumpolar Current and its associated overturning circulation. *J. Phys. Oceanogr.,* **33,** 2341–2354.

——, C. Hill, L. Perleman, and A. Adcroft, 1997a: Hydrostatic, quasi-hydrostatic, and nonhydrostatic ocean modeling. *J. Geophys. Res.,* **102,** 5753–5766.

——, ——, ——, and C. Heisy, 1997b: A finite volume, incompressible Navier–Stokes model for studies of the ocean on parallel computers. *J. Geophys. Res.,* **102,** 5753–5766.

——, H. Jones, R. H. Karsten, and R. Wardle, 2002: Can eddies set ocean stratification? *J. Phys. Oceanogr.,* **32,** 26–38.

McDougall, T. J., and P. C. McIntosh, 1996: The temporal-residual-mean velocity. Part I: Derivation and the scalar conservation equations. *J. Phys. Oceanogr.,* **26,** 2653–2665.

Plumb, R. A., 1979: Eddy fluxes of conserved quantities by small-amplitude waves. *J. Atmos. Sci.,* **36,** 1699–1704.

——, and J. D. Mahlman, 1987: The zonally averaged transport characteristics of the GFDL general circulation/tracer model. *J. Atmos. Sci.,* **44,** 298–327.

——, and R. Ferrari, 2005: Transformed Eulerian-mean theory. Part I: Nonquasigeostrophic theory for eddies on a zonal-mean flow. *J. Phys. Oceanogr.,* **35,** 165–174.

Rhines, P. B., and W. R. Young, 1982: Homogenization of potential vorticity in gyres. *J. Fluid Mech.,* **122,** 347–367.

Treguier, A. M., I. M. Held, and V. D. Larichev, 1997: Parameterization of quasigeostrophic eddies in primitive equation ocean models. *J. Phys. Oceanogr.,* **27,** 567–580.